Synthesis and antimicrobial activity against Pseudomonas aeruginosa of macrocyclic -hairpin peptidomimetic antibiotics containing N-methylated amino acids

Vetterli, Stefan U ; Moehle, Kerstin ; Robinson, John A

Abstract: Antimicrobial resistance among Gram-negative bacteria is a growing problem, fueled by the paucity of new antibiotics that target these microorganisms. One novel family of macrocyclic -hairpin-shaped peptidomimetics was recently shown to act specifically against Pseudomonas spp. by a novel mechanism of action, targeting the outer membrane protein LptD, which mediates lipopolysaccharide transport to the cell surface during outer membrane biogenesis. Here we explore the mode of binding of one of these -hairpin peptidomimetics to LptD in Pseudomonas aeruginosa, by examining the effects on antimicrobial activity following N-methylation of individual peptide bonds. An N-methyl scan of the cyclic peptide revealed that residues on both sides of the -hairpin structure at a non-hydrogen bonding position likely mediate hydrogen-bonding interactions with the target LptD. Structural analyses by NMR spectroscopy further reinforce the conclusion that the folded -hairpin structure of the peptidomimetic is critical for binding to the target LptD. Finally, new NMe analogues with potent activity have been identified, which opens new avenues for optimization in this family of antimicrobial peptides.

DOI: https://doi.org/10.1016/j.bmc.2016.05.027

Synthesis and antimicrobial activity against *Pseudomonas aeruginosa* of macrocyclic ß-hairpin peptidomimetic antibiotics containing N-methylated amino acids

Stefan U. Vetterli, Kerstin Moehle and John A. Robinson

Chemistry Department, University of Zurich, Winterthurerstrasse 190, 8057 Zurich, Switzerland

Author for correspondence:

Professor John A Robinson

Chemistry Department, University of Zurich, Winterthurerstrasse 190, 8057 Zurich, Switzerland

Tel: +41 44 635 4242

E-mail: robinson@oci.uzh.ch

Abstract

Antimicrobial resistance among Gram-negative bacteria is a growing problem, fueled by the paucity of new antibiotics that target these microorganisms. One novel family of macrocyclic ß-hairpin-shaped peptidomimetics was recently shown to act specifically against *Pseudomonas* spp. by a novel mechanism of action, targeting the outer membrane protein LptD, which mediates lipopolysaccharide transport to the cell surface during outer membrane biogenesis. Here we explore the mode of binding of one of these ß-hairpin peptidomimetics to LptD in *P. aeruginosa*, by examining the effects on antimicrobial activity following N-methylation of individual peptide bonds. An N-methyl scan of the cyclic peptide revealed that residues on both sides of the ß-hairpin structure at a non-hydrogen bonding position likely mediate hydrogen-bonding interactions with the target LptD. Structural analyses by NMR spectroscopy further reinforce the conclusion that the folded ß-hairpin structure of the peptidomimetic is critical for binding to the target LptD. Finally, new NMe analogues with potent activity have been identified, which opens new avenues for optimization in this family of antimicrobial peptides.

1. Introduction

The macrocyclic ß-hairpin-shaped peptides shown in Figure 1A represent a new class of antibiotics with potent antimicrobial activity against Gram-negative *Pseudomonas* spp. including the important human pathogen *P. aeruginosa* (PA).[1,2] Their unique mechanism of action involves binding to the outer membrane (OM) protein LptD in PA and inhibition of its essential role in lipopolysaccharide (LPS) transport to the cell surface.[3] Seven essential LPS transport (Lpt) proteins (LptA-G) in Gram-negative bacteria mediate LPS transport from the inner to the OM. After extraction from the inner membrane, LPS travels along a bridge formed by LptA oligomers extending across the periplasm, and is delivered to LptD in the OM, driven by ATP hydrolysis in the cytoplasm (Figure 1B).[4] The function of LptD has been studied most thoroughly in *Escherichia coli*, where in a complex with the lipoprotein LptE it fulfills the final step in the biogenesis of the OM, by translocating LPS molecules delivered by LptA from the periplasmic face into the outer leaflet of the asymmetric OM.[5,6] During exponential growth it has been estimated that in each cell typically ≈1200 LPS molecules per second are exported by LptD to the cell surface during OM biogenesis.[7]

Recently the crystal structure of the full length LptD/E complex from *Shigella flexneri* was reported, which revealed a C-terminal 26-stranded ß-barrel integral membrane domain, conserved in other Gram-negative bacteria, with the lipoprotein LptE enclosed within the ß-barrel (Figure 1C).[8] The ß-barrel domain is inserted in and traverses the OM, while a conserved N-terminal ß-jelly-roll domain in LptD sits underneath in the periplasm and is disulfide-bonded to the ß-barrel. The jelly-roll is

the site to which LPS molecules are delivered to LptD by LptA. The lipoprotein LptE binds inside and acts like a plug in the LptD ß-barrel.

Figure 1. **A**, Peptidomimetics **L27-11** and **LB-01** (Dab = L-2,4-diaminobutyric acid; Orn = L-ornithine). **B**, Schematic view of LPS transport to the OM mediated by the Lpt protein family (see text) (OM = outer membrane; IM = inner membrane; PG = peptidoglycan; PG/PE, phosphatidylglycerol/ethanolamine). **C**, Ribbon representation of the *Shigella flexneri* LptD/E crystal structure from PDB file 4Q35.[8] For LptD, the ß-barrel domain is shown in green/white and the ß-jelly-roll in orange. LptE is light blue.

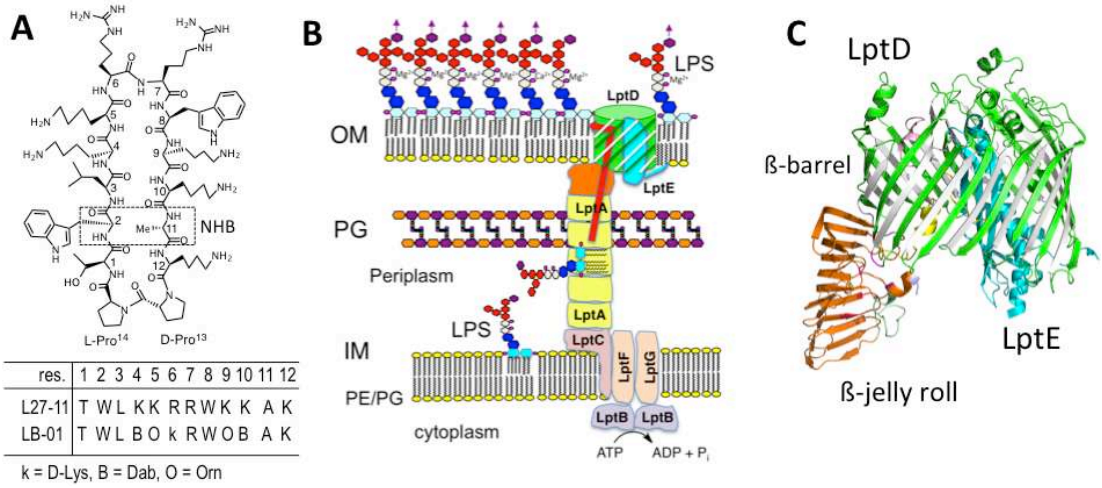

res.	1	2	3	4	5	6	7	8	9	10	11	12
L27-11	T	W	L	K	K	R	R	W	K	K	A	K
LB-01	T	W	L	B	O	k	R	W	O	B	A	K

k = D-Lys, B = Dab, O = Orn

Computational, mutagenesis and photo-crosslinking studies suggest that the lipid chains in LPS move along the hydrophobic cavity in the jelly-roll domain and exit into the outer leaflet of the OM through a transient lateral opening created between ß-strands-1 and -26 in the LptD ß-barrel domain.[9-11] A similar architecture is expected for the LptD/E complex from *P. aeruginosa*, except that sequence comparisons show that an additional ≈90-residue domain of unknown structure and

function is inserted close to the N-terminus of the ß-jelly roll. This insert domain is a distinguishing feature of LptD in *Pseudomonas* spp.

Although the binding site for the peptidomimetic antibiotics in PA LptD has not yet been defined, the ß-hairpin fold of the macrocycle stabilized by a D-Pro-L-Pro template is thought to be important for antibiotic activity.[1] An alanine-scan in the parent compound L27-11 (Figure-1A) showed that the side chains of Trp2 and Trp8, located on opposite faces of the ß-hairpin, are critical for activity.[1] In this work, we explore the importance of individual peptide bonds for antimicrobial activity, by analyzing analogs of LB-01 containing N-methylated amino acid residues. Cross-strand pairs of amino acids in ß-hairpins occupy alternately internal hydrogen-bonding (HB) and non-hydrogen-bonding (NHB) positions.[12] Residue pairs at NHB positions orient their amide NHs and carbonyl COs outward (Figure 1A), where they might engage hydrogen-bonding interactions with a receptor protein. If this occurs, peptide bond N-methylation may disrupt binding and lead to a loss of biological activity. We have used this approach to gain new insights into how the antibiotics interact with LptD, and to search for new analogs with potent antimicrobial activity.

2. Results and Discussion

Synthesis of N-methyl analogs

The synthesis of LB-01 followed a previously described method, in which the linear sequence was assembled on 2-chlorotrityl chloride resin using Fmoc chemistry[13] starting with residue-6, the linear side-chain protected 14-mer peptide was cleaved from the resin with 0.7% TFA, macrocyclization was performed in solution, and

finally all side-chain protecting groups were removed using 95% TFA.[1,14] The twelve N-methylated analogs of LB-01, each containing a single N-methyl residue in the hairpin loop, were prepared in the same way. Some of the necessary protected NMe amino acids were commercially available (Fmoc-NMe-Trp(Boc)-OH, Fmoc-NMe-Leu-OH, Fmoc-NMe-Ala-OH) and could be incorporated using Fmoc chemistry. Other NMe residues were incorporated using the on-resin *Mitsunobu* methylation method developed by Kessler[15] (Figure 2A). For the special case of the Thr1NMe analogue, where coupling of Fmoc-L-Pro-OH onto the resin bound highly hindered NMe-Thr(tBu) gave very low yields, an alternative strategy was used, wherein Fmoc-Pro-NMe-Thr(tBu)-OH dipeptide (**3**) was first prepared, as shown in Figure 2B, and incorporated as a single unit during Fmoc peptide synthesis. All twelve mono N-methylated analogs were obtained after HPLC purification in >95% purity by HPLC (Table 1, and supporting information), for NMR analyses and determination of antimicrobial activity.

Figure 2. Synthesis of the NMe scan library on LB-01. **A**, Overview of the Fmoc-chemistry used for peptide assembly, on-resin N-methylation chemistry and macrocyclization in solution. **B**, synthesis of the dipeptide fragment Fmoc-Pro-NMe-Thr(OtBu)-OH.

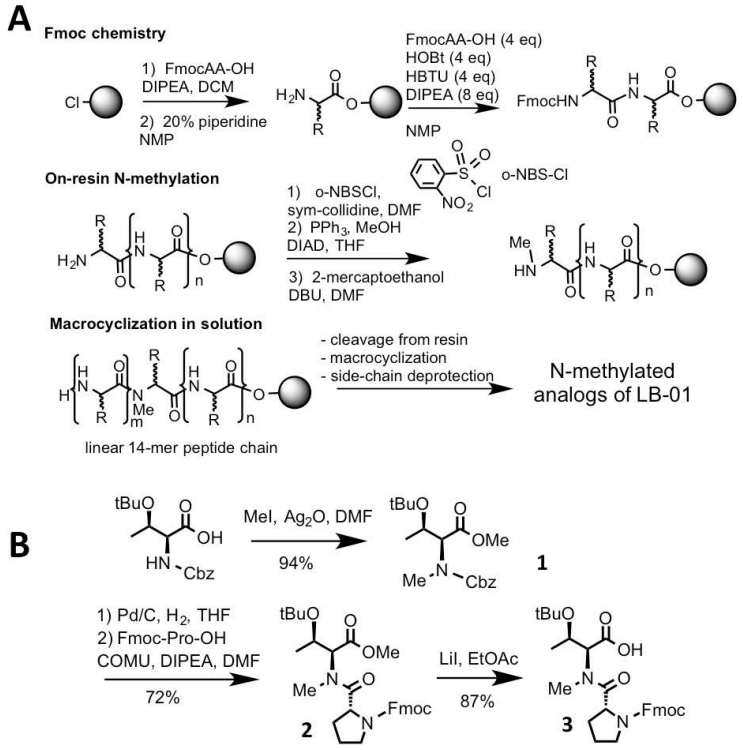

Table 1. NMe scan of LB-01. After purification, each NMe analogue was analyzed by reverse-phase HPLC (t_R retention time (min)) and MS (see supporting information for HPLC chromatograms). Calculated mass and experimental *m/z* values are shown (HPLC, C18 column, with a linear gradient of 10 to 60% MeCN/H_2O+0.1% TFA).

Peptidomimetic	Exact mass (calc.)	m/z (HR-ESI)	t_R (min)
Thr1NMe	1706.02565	854.01996 $[M+2H]^{2+}$	11.4
		569.68292 $[M+3H]^{3+}$	
		427.51393 $[M+4H]^{4+}$	
Trp2NMe	1706.02565	854.02035 $[M+2H]^{2+}$	10.8
		569.68258 $[M+3H]^{3+}$	
		427.51382 $[M+4H]^{4+}$	
Leu3NMe	1706.02565	854.01884 $[M+2H]^{2+}$	12.6
		569.68228 $[M+3H]^{3+}$	
		427.51364 $[M+4H]^{4+}$	
Dab4NMe	1706.02565	854.01946 $[M+2H]^{2+}$	10.9
		569.68196 $[M+3H]^{3+}$	
		427.51310 $[M+4H]^{4+}$	
Orn5NMe	1706.02565	854.02013 $[M+2H]^{2+}$	12.0
		569.68328 $[M+3H]^{3+}$	
		427.51416 $[M+4H]^{4+}$	
^{D}Lys6NMe	1706.02565	854.01956 $[M+2H]^{2+}$	10.6
		569.68207 $[M+3H]^{3+}$	
		427.51349 $[M+4H]^{4+}$	
Arg7NMe	1706.02565	854.01911 $[M+2H]^{2+}$	11.7
		569.68236 $[M+3H]^{3+}$	
		427.51394 $[M+4H]^{4+}$	
Trp8NMe	1706.02565	854.01905 $[M+2H]^{2+}$	11.4
		569.68204 $[M+3H]^{3+}$	
		427.51330 $[M+4H]^{4+}$	
Orn9NMe	1706.02565	854.02048 $[M+2H]^{2+}$	12.1
		569.68328 $[M+3H]^{3+}$	
		427.51441 $[M+4H]^{4+}$	
Dab10NMe	1706.02565	854.01930 $[M+2H]^{2+}$	11.3
		569.68200 $[M+3H]^{3+}$	

		427.51286 $[M+4H]^{4+}$	
Ala11NMe	1706.02565	854.01880 $[M+2H]^{2+}$ 569.68178 $[M+3H]^{3+}$	11.0
		427.51305 $[M+4H]^{4+}$	
Lys12NMe	1706.02565	854.01921 $[M+2H]^{2+}$ 569.68255 $[M+3H]^{3+}$	12.9
		427.51400 $[M+4H]^{4+}$	

Antimicrobial activity

Minimum Inhibitory Concentrations (MICs) were determined by the microbroth dilution method in a microtitre plate format in Mueller-Hinton-I broth, using two *P. aeruginosa* strains. The results shown in Figure 3 reveal dramatic differences in antimicrobial activity against both strains within the NMe scan library. Notable is the complete loss in activity after N-methylation of residues on the lower part (proximal to the D-Pro-L-Pro template) on both sides of the predicted hairpin structure (residues 2, 3, 11 or 12) and major losses in activity after N-methylation of Orn9 and Dab10. However, N-methylation of residues on the upper part, or tip of the hairpin (residues 4, 5 , 6 and 8) largely retain or even show slightly improved activity compared to LB-01. Overall, methylations in the ß-strand residues 1-5 result in large variations in activity. However, the N-methylation of the backbone of most of the second ß-strand (residues 9-11), strongly affects antimicrobial activity. The Thr1NMe analogue retains significant activity, which is remarkable given its location so close to the D-Pro-L-Pro template and the strong H-bonding interaction between the Thr1NH and the carbonyl of residue-12, seen in the NMR structure of LB-01.[1]

Figure 3. Antimicrobial activity (MIC, μg/mL) of the NMe scan library on LB-01.

peptide	MIC (µg/mL) PA ATCC27853	PA PAO1
LB-01	0.008	0.015
Thr1NMe	0.19	0.38
Trp2NMe	>64	>64
Leu3NMe	>64	>64
Dab4NMe	0.005	0.009
Orn5NMe	0.009	0.008
DLys6NMe	0.012	0.025
Arg7NMe	0.38	0.75
Trp8NMe	0.023	0.13
Orn9NMe	12	16
Dab10NMe	1	12
Ala11NMe	>64	>64
Lys12NMe	>64	>64

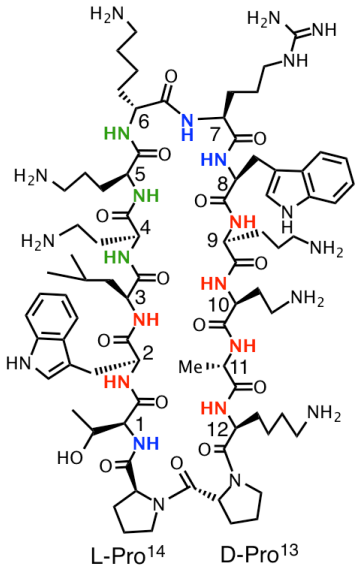

LB-01

A more detailed analysis of these structure-activity relationships now rests upon an understanding of how each N-methylation affects the folded ß-hairpin conformation of the macrocycle, which in LB-01 is characterized by two regular ß-strands (residues 1-5 and 8-12) and stable type-II' ß-turns in the template and at the hairpin tip (residues 6 and 7).[1]

NMR Studies and SAR

The cyclic peptide LB-01 is a single rotamer (>98%) in aqueous solution with all peptide bonds *trans*.[1] The backbone adopts a stable folded ß-hairpin conformation according to several NMR criteria, including $^{3}J_{HNH\alpha}$ values ≥8.0 Hz typical of residues in the ß-region of ϕ/ψ-space;[16] mostly positive NMR chemical shift deviations (CSDs) ($\Delta\delta = \delta_{observed} - \delta_{random}$) for Hα indicative of regular ß-structure;[17,18] and a network of long range cross-strand NOEs in 2D NOESY plots characteristic of a folded ß-hairpin

structure. Both the tip region (DLys^{6}-Arg^{7}) and the template (DPro^{13}-LPro^{14}) in LB-01 adopt stable type-II' ß-turn structures.[1]

cis-trans conformational isomers (rotamers)

Whereas several of the NMe analogues exist predominantly (≥95%) with all-*trans* peptide bonds, both at the site of N-methylation and at the Lys12-D-Pro13 peptide bond, the situation becomes more complex for some others (Table 2). The Trp8NMe analogue exists as 1:1 *trans-cis* at Arg7-TrpNMe8 and the Leu3NMe analogue as 3:1 *trans-cis* at Trp2-Leu3NMe. Both Orn9NMe and Dab10NMe analogues show resonances for *cis-trans* rotamers at both the site of methylation and at D-Pro13, indicating an even more complex conformational behavior in these macrocycles.

Trp2NMe and Ala11NMe

Table 2. Occurrence of *cis-trans* peptide bond rotamers in peptides detected by ^{1}H-NMR.

peptide	*cis rotamers (%)*	*amide bonds*
LB-01	< 5%	
Thr1NMe	7%	LPro-Thr1NMe
Trp2NMe	7%	Thr1-Trp2NMe
Leu3NMe	25%	Trp2-Leu3NMe
Dab4NMe	5%	Leu3-Dab4NMe
Orn5NMe	< 5%	
DLys6NMe	< 5%	
Arg7NMe	< 5%	
Trp8NMe	50 %	Arg7-Trp8NMe
Orn9NMe	25%, 12%	Trp8-Orn9NMe, Lys12-DPro13
Dab10NMe	25%, 8%	Orn9-Dab10NMe Lys12-DPro13
Ala11NMe	8%	Dab10-Ala11NMe
Lys12NMe	10%	Ala11-Lys12NMe

Two of the four analogues that completely lose activity (Trp2NMe and Ala11NMe; Figure 3) are at a cross-strand NHB position with their NH(or Me) groups oriented outwards. Yet both these NMe analogues retain a folded ß-hairpin structure in solution. This is apparent from the numerous cross-strand NOEs seen in NOESY plots of each analogue, the mostly positive CSDs characteristic of Hα protons and $^{3}J_{HN^{\alpha}}$ values ≥8.0 Hz, both typical of residues in the ß-region of ϕ/ψ-space (Figure 4A-C). Structure calculations using NOE-derived distance restraints yielded average solution structures for the Ala11NMe and Trp2NMe analogues, with well-defined ß-hairpin backbones (shown in Figure 4D). Hence the loss in activity in both is not caused by a loss of the folded ß-hairpin backbone structure. Rather, the results provide evidence that both amide NH groups of Trp2 and Ala11 make critical contacts to the receptor LptD, which are disrupted by N-methylation. An alternative explanation, that N-methylation might prevent permeation to the binding site on LptD seems less likely, since LptD is exposed to the medium in the OM.

Leu3NMe and Lys12NMe

The Leu3NMe and Lys12NMe analogues also have no activity, which can be explained by the NH groups in these two amino acids being involved in internal hydrogen bonds in the parent peptide (Figure 3). Signal overlap in their ^{1}H-NMR spectra precluded a detailed analysis of the *cis*-rotamers (Table 2), but the minor occurrence of *cis* rotamers cannot alone account for the complete loss in antimicrobial activity seen for both. More telling, ^{1}H NOESY data reveal for the *trans* rotamers NOEs that cannot be reconciled with regular ß-hairpin structures (Figure 4A). A network of cross-strand NOEs characteristic of folded ß-hairpin conformations are not seen. In addition, $^{3}J_{HN^{\alpha}}$ values <8.0 Hz, and CSDs uncharacteristic of ß-structure

(Figure 4B/C), all suggest that quite different backbone conformations are present. We speculate that the loss of ß-hairpin structure is likely due to loss of cross-strand H-bonding interactions, likely combined with deleterious cross-strand steric interactions when the new NMe groups are present. A similar complete loss of antimicrobial activity correlating with loss of ß-hairpin structure was observed earlier in another analogue of LB-01 in which the D-Pro^{13}-L-Pro^{14}-template was changed to L-Pro^{13}-D-Pro^{14}.[1]

Orn9NMe and Dab10NMe

The Orn9NMe and Dab10NMe analogues retain weak antimicrobial activity. Orn9 is at a NHB position in the LB-01 ß-hairpin, whereas Dab10 is at an internal HB position. Only a few long range NOEs are seen in NOESY plots for each analogue, and some observed NOEs are not compatible with stable regular ß-hairpin structures (Figure 4A). The pattern of CSDs observed for both also indicate non-ß backbone conformers. We must conclude, therefore, that weak activity in these two analogues (compared to LB-01) could be due to steric hindrance from the new NMe group upon receptor binding and/or changed (i.e. non-ß-hairpin) global backbone macrocycle conformations.

Other NMe analogues

The remaining analogues (Thr1NMe, Dab4NMe, Orn5NMe, DLys6NMe, Arg7NMe, Trp8NMe) all retain significant antimicrobial activity, which in the case of Dab4NMe and Orn5NMe are comparable or even slightly improved compared to LB-01 (Figure-3).

Figure 4. NMR studies. **A**, long range NOEs observed in NOESY plots for the analogues shown. **B**, coupling constants ($^3J_{HNH\alpha}$, Hz) for selected analogues discussed in the text. **C**, chemical shift deviations (CSDs) ($\Delta\delta = \delta_{observed} - \delta_{random}$) of Hα resonances of residues 1-12 in selected analogues. Positive values are expected for residues in ideal ß-structure. **D**, Average NMR backbone structures (side chains omitted for clarity) for selected analogues; 20 selected structures and one typical structure for Thr1NMe are shown. For each, the D-Pro-L-Pro template and residue number is indicated (compare **A**); N atoms in blue; O-atoms in red.

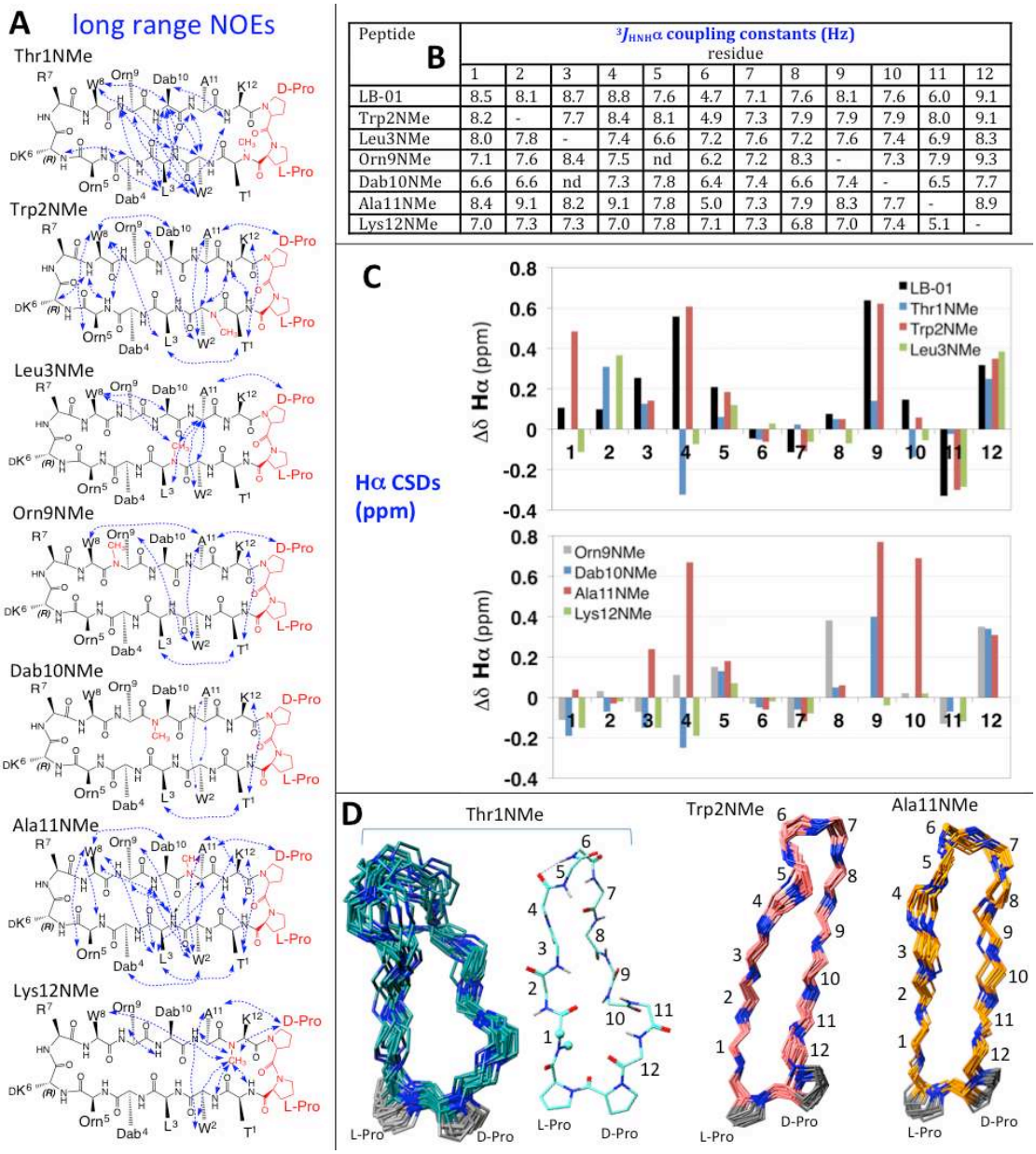

Peptide	$^3J_{HNH\alpha}$ coupling constants (Hz) residue											
B	1	2	3	4	5	6	7	8	9	10	11	12
LB-01	8.5	8.1	8.7	8.8	7.6	4.7	7.1	7.6	8.1	7.6	6.0	9.1
Trp2NMe	8.2	-	7.7	8.4	8.1	4.9	7.3	7.9	7.9	7.9	8.0	9.1
Leu3NMe	8.0	7.8	-	7.4	6.6	7.2	7.6	7.2	7.6	7.4	6.9	8.3
Orn9NMe	7.1	7.6	8.4	7.5	nd	6.2	7.2	8.3	-	7.3	7.9	9.3
Dab10NMe	6.6	6.6	nd	7.3	7.8	6.4	7.4	6.6	7.4	-	6.5	7.7
Ala11NMe	8.4	9.1	8.2	9.1	7.8	5.0	7.3	7.9	8.3	7.7	-	8.9
Lys12NMe	7.0	7.3	7.3	7.0	7.8	7.1	7.3	6.8	7.0	7.4	5.1	-

The Thr1NMe analogue is of special interest, since in LB-01 the D-Pro-L-Pro template is expected to direct the Thr1NH into a hydrogen-bonding interaction with the Lys12 carbonyl group. However, in the Thr1NMe analogue, the NMe group must be oriented away from the Lys12 CO to avoid a steric clash. Nevertheless, the Thr1NMe analogue shows a large number of cross-strand NOEs. Calculated structures for this analogue (Figure 4D) suggest that a distortion from regular ß-structure must occur in the critical segment of the backbone close to the template, which most likely also explains the reduced antimicrobial activity of this analogue.

The remaining analogues, with NMe groups in the tip region retain excellent antimicrobial activity and hence an ability to interact with the target LptD. Only the Arg7NMe analogue suffers a ≈50 fold reduction in the MIC, possibly due to steric clashes between LptD and the hairpin tip. The outward-facing backbone NH groups of Dab4 and DLys6 largely retain antimicrobial activity upon N-methylation and so are unlikely to directly mediate contacts to LptD. Clearly, the inward facing Orn5 NH can also readily accommodate N-methylation upon interaction with LptD.

3. Conclusions

Almost all OM proteins in Gram-negative bacteria are rich in ß-structure, as seen in the ß-barrel and ß-jelly-roll domains of LptD from *S. flexneri* (Figure 1C). Ligands containing folded ß-hairpin structures might be well suited to interact with such ß-rich proteins through antiparallel strand-strand interactions, as illustrated in Figure 5. One intriguing possibility is that binding of the antibiotics occurs to transient LptD structures that arise during LPS transport to the bacterial cell surface. LptD along with several other OM proteins in Gram-negative bacteria are believed to transport substrates into the membrane through lateral gates formed by transient opening of the

Figure 5. The folded ß-hairpin structure of LB-01 and possible interactions with neighboring ß-strands in the target protein LptD (in bold). Dotted lines indicate H-bonding interactions between LB-01 and LptD suggested by the NMe-scan.

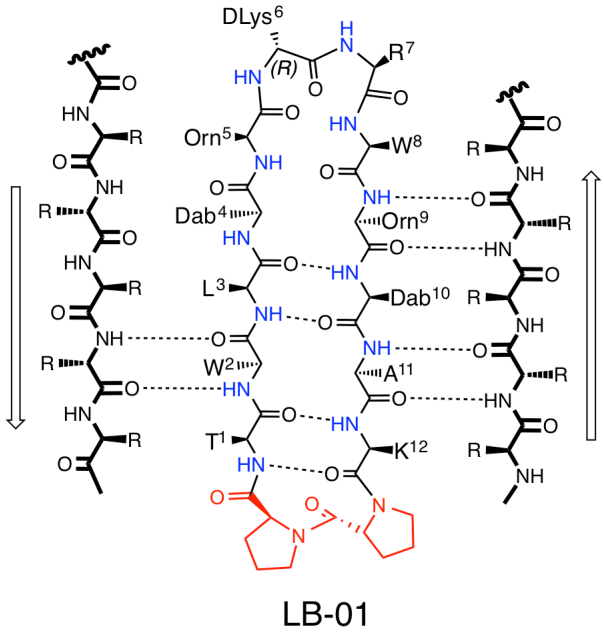

first and last ß-strands in the ß-barrel.[8,9,11,19,20] Such complex dynamic processes might create a binding site for the antibiotic between antiparallel ß-strands, allowing H-bonding interactions to both sides of the antibiotic ß-hairpin (Figure 5). Access to such a binding site might also be possible from the cell exterior, following initial electrostatic attraction of the cationic antibiotic to anionic LPS molecules in the outer leaflet. The results described here provide some support for such a binding mode, by showing that outward-facing peptide NH groups on both sides of the ß-hairpin structure of LB-01 are sensitive to N-methylation, in particular, N-methylation of Trp2, Ala11 and Orn9 leads to major losses of antimicrobial activity. Moreover, whenever N-methylation at other positions leads to disruption of the folded ß-hairpin structure, large losses of antimicrobial activity are also observed, reinforcing the

conclusion from earlier studies[1] that the regular ß-hairpin structure is crucial for optimal antimicrobial activity and binding to LptD.

4. Experimental Section

Peptide synthesis. Peptides were assembled on 2-chlorotrityl chloride resin with Fmoc chemistry on a 0.25 mmol scale with an *Applied Biosystems* ABI433A synthesizer and a Perkin-Elmer785A UV/VIS detector for reaction monitoring. Couplings were performed with HBTU/HOBt (4 eq.) in NMP and DIPEA (8 eq.), and Fmoc deprotection was with 20% piperidine in NMP. Macrocyclization in solution was performed as described earlier.[14] Analytical HPLC was performed on an *Amersham* Aekta Purifier 100 system with an *Agilent* C18 4.6 × 250 mm column with 5 μm particle size (1 mL/min), and a C18 21.2 × 250 mm column with 7 μm particle size on preparative scale (17 mL/min). Linear gradients ranged from 10 to 60% MeCN/H_2O with 0.1% TFA. High-resolution electrospray ionization spectra (HR-ESI) were recorded using a *Bruker* MaXis spectrometer (accuracy ±1ppm). ^{1}H-, ^{13}C- and 2D-NMR spectra were recorded on Bruker AV-400 or AV-600 instruments at room temperature. Chemical shifts (δ) are reported in ppm and are referenced to TMS or TSP (0 ppm) as internal standard.

(2*S*,3*R*)-Methyl-2-(((benzyloxy)carbonyl)(methyl)amino)-3-(tert-butoxy)butanoate (1)

Z-Thr(tBu)-OH dicylohexylamine salt (1.00 g, 2.04 mmol) was converted to the free acid by treatment with aq. citric acid 5% and extraction into Et_2O (3 x 20 ml). Ag_2O (1.89 g, 8.16 mmol) was added to a solution of *Z*-Thr(tBu)-OH free acid and MeI

(1.91 ml, 30.6 mmol) in DMF (7 ml) and stirred overnight at room temperature. CH_2Cl_2 (15 mL) was then added and the solution was filtered through celite. The filter cake was washed with CH_2Cl_2 (3 x 20 mL), and the combined organic phases were washed with 15% aq. $Na_2S_2O_3$ (2 x 30 mL), water (3 x 30mL) and brine (30 mL). After drying ($MgSO_4$) the combined organic phases were concentrated in vacuo and the oily residue was purified by flash column chromatography (4:1 cyclohexane/EtOAc) yielding 647 mg of colourless oil (**1**) (94% yield). TLC (silica): Rf 0.50 (hexane/EtOAc 4:1). $[\alpha]_D^{24}$: +3.5° (c 0.65, MeOH). ^{1}H-NMR ($CDCl_3$): two rotamers with an approx. 2:1 ratio. Major: δ =7.39 – 7.27 (m, 5H), 5.21 – 5.04 (m, 2H), 4.82 (d, J=4.3 Hz, 1H), 4.41-4.35 (m, 1H), 3.70 (s, 3H) 3.14 (s, 3H), 1.86 (d, J=6.2 Hz, 3H), 1.28 (s, 9H). Minor: δ =7.39 – 7.27 (m, 5H), 5.21 – 5.04 (m, 2H), 4.59 (d, J= 5.1 Hz, 1H), 4.30-4.24 (m, 1H), 3.65 (s, 3H), 3.11 (s, 3H), 1.58 (d, J=6.2 Hz, 3H), 1.12 (s, 9H). ^{13}C-NMR ($CDCl_3$): Major: δ = 170.7, 157.6, 136.8, 128.5, 128.0, 127.9, 127.6, 74.0, 68.4, 67.4, 64.1, 51.7, 33.6, 28.7, 20.5. Minor: δ = 170.5, 156.4, 136.6, 128.5, 128.0, 127.9, 127.6, 74.1, 67.9, 67.4, 64.4, 51.7, 34.1, 28.7, 20.7. HR-ESI: calc. for $C_{22}H_{25}NNaO_4$ $[M+Na]^+$ 390.1676, found 390.1672.

(*R*)-(9H-Fluoren-9-yl)methyl 2-(((2*S*,3*R*)-3-(tert-butoxy)-1-methoxy-1-oxobutan-2-yl) (methyl)carbamoyl)pyrrolidine-1-carboxylate (2)

To the foregoing dipeptide (**1**) (294 mg, 0.87 mmol) in THF (9 mL) was added Pd/C (10%, 93 mg, 0.09 mmol), and stirred for 30 min under H_2. The solution was then filtered through celite, washed with THF and dried under vacuo. COMU (746 mg, 1.74 mmol) was added to a mixture of Fmoc-Pro-OH (588 mg, 1.74 mmol), the dipeptide and DIPEA (445 μl, 2.61 mmol) in DMF (9 ml) at 0°C. The reaction mixture was warmed to RT and stirred for 2 h. The mixture was then diluted with

EtOAc (25 ml) and washed with aq. citric 5% (2 x 15 ml), 1M $NaHCO_3$ (2 x 15 ml) and saturated NaCl (2 x 15 ml). The organic layer was then dried over $MgSO_4$ and the solvent removed in vacuo. The residue was purified by flash column chromatography (2:1 (v/v) cyclohexane/EtOAc then 1:1 (v/v) cyclohexane/EtOAc), to give **2** yield: 327 mg reddish foam that solidified overnight (72% yield). TLC: R_f 0.47 (cyclohexane/EtOAc, 1:1). M.p. 64 - 68 °C. $[\alpha]_D^{24}$: -42.3 ° (c 0.22, MeOH). ^{1}H-NMR ($CDCl_3$): Two rotamers with approx. 2:1 ratio, each with a low abundance rotamer from the *N*-methyl-amide (not assigned). ^{1}H-NMR ($CDCl_3$): Major: δ = 7.78 - 7.73 (m, 2H), 7.67 - 7.55 (m, 2H), 7.42 - 7.35 (m, 2H), 7.34 - 7.27 (m, 2H), 5.35 (s, J = 3.5 Hz, 1H), 4.86 (dd, J = 8.4 Hz, 1H), 4.47 - 4.41 (m, 1H), 4.41 - 4.37 (m, 1H), 4.33 - 4.26 (m, 1H), 4.30 - 4.24 (m, 1H), 3.70 (s, 3H), 3.80 - 3.72 (m, 1H), 3.62 - 3.56 (m, 1H), 3.34 (s, 3H), 2.30 - 2.21 (m, 1H), 2.05 - 1.96 (m, 1H), 2.20 - 2.09 (m, 1H), 2.03 - 1.92 (m, 1H), 1.20 (d, J = 6.3 Hz, 3H), 1.14 (s, 9H). Minor: δ = 7.78 - 7.73 (m, 2H), 7.67 - 7.55 (m, 2H), 7.42 - 7.35 (m, 2H), 7.34 - 7.27 (m, 2H), 5.29 (s, J = 3.5 Hz, 1H), 4.65 (dd, J = 8.4 Hz, 1H), 4,71 - 4.65 (m, 1H), 4.41 - 4.35 (m, 1H), 4.23 - 4.16 (m, 1H), 4.21 - 4.16 (m, 1H), 3.68 (s, 3H), 3.69 - 3.63 (m, 1H), 3.56 - 3.47 (m, 1H), 3.15 (s, 3H), 2.30 - 2.21 (m, 1H), 2.02 - 1.95 (m, 1H), 2.04 - 1.96 (m, 1H), 2.91 - 1.82 (m, 1H),1.09 (s, 9H), 0.93 (d, J = 6.3 Hz, 3H). ^{13}C-NMR (100 MHz): Major: δ = 174.1, 170.7, 154.8, 144.3, 144.0, 141.3, 127.6, 127.0, 125.4, 125.2, 119.9, 74.0, 68.8, 67.4, 61.5, 57.0, 51.7, 47.2, 47.6, 34.4, 29.2, 28.7, 24.3, 20.3. Minor: δ = 173.9, 170.5, 154.3, 144.4, 143.9, 141.3, 127.6, 127.1, 127.0, 125.3, 125.1, 119.9, 119.8, 74.1, 68.5, 66.9, 61.4, 56.8, 51.7, 47.4, 46.9, 34.0, 30.2, 28.7, 23.0, 20.2. HR-ESI: calculated for $C_{22}H_{25}NNaO_4$ $[M+Na]^+$ 390.1676, found 390.1672.

(2*S*,3*R*)-2-((R)-1-(((9H-Fluoren-9-yl)methoxy)carbonyl)-N-methylpyrrolidine-2-carboxamido)-3-(tert-butoxy)butanoic acid (3)

To the foregoing methyl ester (**2**) (265 mg, 0.51 mmol) in EtOAc (5 mL) was added LiI (679 mg, 5.07 mmol). The mixture was refluxed for 16 h. After cooling, water was added and the solution acidified with aq. citric acid 5% to pH 3, and extracted with EtOAc (3 x 20 ml). The combined organic phases were dried over $MgSO_4$ and concentrated in vacuo. The product (**3**) was purified by flash column chromatography (19:1 to 4:1 v/v CH_2Cl_2/MeOH) yielding 203 mg of a white solid (79% yield). M.p. 96 - 99 °C. TLC: Rf : 0.51 (9:1 CH_2Cl_2/MeOH). $[\alpha]_D^{24}$: -34.8° (c 0.23, MeOH)

Two rotamers with an approximate ratio of 1:1 (Fmoc-amide rotation) are apparent by NMR, each with a low abundance rotamer deriving from the *N*-methyl-amide (not assigned). ^{1}H-NMR (DMSO-d_6): Rotamer 1: δ = 12.80 - 12.62 (br, 1H), 7.92 - 7.85 (m, 2H), 7.70 - 7.53 (m, 2H), 7.45- 7.39 (m, 2H), 7.37 - 7.26 (m, 2H), 4.79 (d, J=3.7 Hz, 1H), 4.75 - 4.68 (m, 1H), 4.38 - 4.34 (m, 1H), 4.27 - 4.21 (m, 2H), 4.17 - 4.11 (m, 1H), 3.49-3.39 (m, 2H), 3.16 (s, 3H), 2.32 - 2.18 (m, 1H), 1.83 - 1.76 (m, 2H), 1.79 - 1.73 (m, 1H), 1.12 (s, 9H), 1.04 (d, J = 6.3 Hz, 3H). Rotamer 2: δ = 12.80 - 12.62 (br, 1H), 7.92 - 7.85 (m, 2H), 7.70 - 7.53 (m, 2H), 7.45 - 7.39 (m, 2H), 7.37 - 7.26 (m, 2H), 5.01 (d, J = 3.7Hz, 1H), 4.75 - 4.68 (m, 1H), 4.44 - 4.38 (m, 1H), 4.34 - 4.29 (m, 1H), 4.28 - 4.23 (m, 1H), 4.14 - 4.07 (m, 1H), 3.49 - 3.39 (m, 2H), 3.08 (s, 3H), 2.32 - 2.18 (m, 1H), 1.91 - 1.83 (m, 2H), 1.75 - 1.69 (m, 1H), 1.06 (s, 9H), 0.88 (d, J = 6.3 Hz, 3H). ^{13}C-NMR (DMSO-d_6): Rotamer 1: δ =172.9, 171.5, 153.6, 143.9, 143.8, 140.7, 127.6, 127.1, 125.2, 120.1, 73.2, 67.9, 66.4, 61.2, 56.6, 47.1, 46.9, 33.7, 29.6, 28.5, 23.7, 20.5. Rotamer 2: δ = 172.8, 171.3, 153.6, 143.8, 143.4, 140.7, 127.6, 127.1, 125.1, 120.0, 73.2, 67.8, 66.2, 60.9, 56.4, 46.6, 46.4, 33.6, 28.6, 28.5, 23.7, 20.3. HR-ESI: calculated for $C_{29}H_{36}N_2NaO_6$ $[M+Na]^+$ 531.24715, found 531.24656.

NMR structure calculations

^{1}H NMR spectra were measured in H_2O/D_2O (9:1) or pure D_2O at pH 3 on a Bruker AV-600 spectrometer at 300 K. Water suppression was performed by presaturation. Spectral assignments were made using standard methods from 2D DQF-COSY, TOCSY and NOESY spectra. $^{3}J_{HNH\alpha}$ coupling constants were determined from 1D spectra or in the case of signal overlap from 2D NOESY spectra by inverse Fourier transformation of in-phase multiplets. Spectra were typically collected with 1024 x 256 complex data points zero-filled prior to Fourier transformation to 2048 x 1024, and transformed with a cosine-bell weighting function. Distance restraints were obtained from NOESY spectra with a mixing time of 250 ms. The structure calculations were performed by restrained molecular dynamics in torsion angle space by applying the simulated annealing protocol implemented in the program CYANA.[21] Starting from 100 randomized conformations a bundle of 20 conformations is selected, which incur the lowest CYANA target energy function (see Supporting information). MOE (*Chemical Computing Group*, Quebec, Canada) was used for structure analysis and visualization of the molecular models.

Acknowledgements

We thank Annelies Meier and Myriam Gwerder for assistance in measurement of MIC values, and the Swiss National Science Foundation for financial support.

Supplementary data

Supplementary data associated with this article can be found in the online version at http://dx.doi.org/.....

References and notes

1 Schmidt, J.; Patora-Komisarska, K.; Moehle, K.; Obrecht, D.; Robinson, J. A. *Bioorg. Med. Chem.* **2013**, *21*, 5806.

2 Srinivas, N.; Jetter, P.; Ueberbacher, B. J.; Werneburg, M.; Zerbe, K.; Steinmann, J.; Van der Meijden, B.; Bernardini, F.; Lederer, A.; Dias, R. L. A.; Misson, P. E.; Henze, H.; Zumbrunn, J.; Gombert, F. O.; Obrecht, D.; Hunziker, P.; Schauer, S.; Ziegler, U.; Kach, A.; Eberl, L.; Riedel, K.; DeMarco, S. J.; Robinson, J. A. *Science* **2010**, *327*, 1010.

3 Werneburg, M.; Zerbe, K.; Juhas, M.; Bigler, L.; Stalder, U.; Kaech, A.; Ziegler, U.; Obrecht, D.; Eberl, L.; Robinson, J. A. *Chembiochem* **2012**, *13*, 1767.

4 Putker, F.; Bos, M. P.; Tommassen, J. *FEMS Microbiol. Rev.* **2015**, *39*, 985.

5 May, J. M.; Sherman, D. J.; Simpson, B. W.; Ruiz, N.; Kahne, D. *Phil. Trans. Roy. Soc. B.* **2015**, *370*, 7.

6 Simpson, B. W.; May, J. M.; Sherman, D. J.; Kahne, D.; Ruiz, N. *Phil. Trans. Roy. Soc. B.* **2015**, *370*, 8.

7 Whitfield, C.; Trent, M. S. *Annu. Rev. Biochem.* **2014**, *83*, 99.

8 Qiao, S.; Luo, Q. S.; Zhao, Y.; Zhang, X. J. C.; Huang, Y. H. *Nature* **2014**, *511*, 108.

9 Dong, H. H.; Xiang, Q. J.; Gu, Y. H.; Wang, Z. S.; Paterson, N. G.; Stansfeld, P. J.; He, C.; Zhang, Y. Z.; Wang, W. J.; Dong, C. J. *Nature* **2014**, *511*, 52.

10 Gu, Y. H.; Stansfeld, P. J.; Zeng, Y.; Dong, H. H.; Wang, W. J.; Dong, C. J. *Structure* **2015**, *23*, 496.

11 Li, X. J.; Gu, Y. H.; Dong, H. H.; Wang, W. J.; Dong, C. J. *Scient. Rep.* **2015**, *5*, 8.

12 Robinson, J. A. *Accts. Chem. Res.* **2008**, *41*, 1278.

13 Atherton, E.; Sheppard, R. C. *Solid phase peptide synthesis: A practical approach*; Oxford University Press: Oxford, UK, 1989.

14 Jiang, L.; Moehle, K.; Dhanapal, B.; Obrecht, D.; Robinson, J. A. *Helv. Chim. Acta* **2000**, *83*, 3097.

15 Chatterjee, J.; Laufer, B.; Kessler, H. *Nat. Protocols* **2012**, *7*, 432.

16 Wüthrich, K. *NMR of Proteins and Nucleic Acids*; John Wiley & Sons: New York, 1986.

17 Fesinmeyer, R. M.; Hudson, F. M.; Olsen, K. A.; White, G. W. N.; Euser, A.; Andersen, N. H. *J. Biomol. NMR* **2005**, *33*, 213.

18 Wishart, D. S. *Prog. Nucl. Mag. Res. Spectr.* **2011**, *58*, 62.

19 Lepore, B. W.; Indic, M.; Pham, H.; Hearn, E. M.; Patel, D. R.; van den Berg, B. *Proc. Natl. Acad. Sci. USA* **2011**, *108*, 10121.

20 Noinaj, N.; Kuszak, A. J.; Balusek, C.; Gumbart, J. C.; Buchanan, S. K. *Structure* **2014**, *22*, 1055.

21 Güntert, P. *Meth. Mol. Biol.* **2004**, *278*, 353.